Statistical Analysis of Vibration Modes of a Suspension Bridge Using Spatially Dense Wireless Sensor Network

Shamim N. Pakzad[1] and Gregory L. Fenves[2]

Abstract: A spatially dense wireless sensor network was designed, developed and installed on a long-span suspension bridge for a 3-month deployment to record ambient acceleration. A total 174 sets of data (1.3 GB) were collected from 64 sensor nodes on the main span and south tower of the Golden Gate Bridge. Analysis of the vibration data using power spectral densities and peak picking provide approximate estimates of vibration modes with minimal computation. For more detailed analysis of the data, autoregressive with moving average models (ARMA) give parametric estimates of vibration modes for frequencies up to 5 Hz. Statistical analysis of the multiple realizations give the distributions of the vibration frequencies, damping ratios, and mode shapes and 95% confidence intervals. The statistical results are compared with vibration properties using the peak picking method and previous studies of the bridge using measured data and a finite-element model. Analysis of the ambient vibration data and system identification results demonstrate that high spatial and temporal sensing using the wireless sensor network give a high resolution and confidence in the identified vibration modes. The estimation errors for the identified vibration properties are generally low, with frequencies being the most accurate and damping ratios the least accurate.

DOI: 10.1061/(ASCE)ST.1943-541X.0000033

CE Database subject headings: Bridges, suspension; Statistics; Probe instruments; Monitoring; Modal analysis; Vibration.

Introduction

With the rapid development of wireless sensor technology, the number of sensor nodes in a network for monitoring a structure may be increased by orders of magnitude compared with traditional sensors tethered by communication cables. Tethered (or wired) sensor networks on a major structure, such as a long-span bridge, have been limited by the number of nodes because of the expense of cabling. In comparison the high spatial density possible with the new generation of wireless sensor networks produces more detailed data that can be used to identify higher vibration modes and localized features of structural response. The ability to capture multiple realizations of structural response allows estimates of statistical confidence and repeatability.

Sensor networks of different kinds, but most commonly using accelerometers, have been deployed on long-span bridges and used for estimating vibration properties. Abdel-Ghaffar et al. (1995); Grimmelsman et al. (2007); Niazy (1991); Fujino et al. (2000); Jones and Spartz (1990); Brownjohn et al. (1989, 1992); Chang et al. (2001); Cunha et al. (2001); Smyth et al. (2003); Lu et al. (2006); and He et al. (2005) present studies of long-span bridges using data from tethered or wireless sensor networks. The spatial density of these networks was generally sparse, usually limited to fewer than 20 sensing locations, and only a few data sets were recorded. This restricts the number of identified modes and makes it difficult to identify the higher vibration modes. The limited number of realizations documented in the previous studies does not allow a statistical analysis of the confidence in the vibration properties.

To address these issues, the objective of this paper is to present a statistical analysis of the vibration modes of a suspension bridge using ambient acceleration data obtained from large-scale deployment of a wireless sensor network. The contribution is to demonstrate that the spatial and temporal sensing possible with wireless sensor networks (WSNs) provides high resolution and confidence in the identified vibration modes. As a distinguished long-span bridge (Strauss 1937; Stahl et al. 2007), the Golden Gate Bridge has been the subject of several instrumentation studies and is also the subject of this study using a WSN. The U.S. Coast and Geodetic Survey installed seismological sensors on the piers, towers, deck and cables between 1933 and 1942 at different stages of construction and initial operation (Vincent 1958). Ten vertical accelerometers were installed in 1945 and operated until 1954 (Vincent 1958, 1962). Abdel-Ghaffar and Scanlan (1985a,b) performed the most recent ambient vibration study using accelerometers on the main span and south tower.

In contrast with the earlier studies, WSN in the present study has much higher spatial resolution and the ambient vibration data are collected over an extended period of time, which allows statistical analysis. The statistical approach demonstrated in this paper is applicable to sensor networks on other bridges and buildings, and can be used as a template for analysis of systems with streaming data. The calibration of a finite-element model for the bridge is beyond the scope of this paper, but the statistical properties of the vibration mode shapes, including higher modes, may be used for calibration in future work. The first section of the paper describes the deployment of a wireless sensor network on the Golden Gate Bridge. The second section presents an analysis

[1]Assistant Professor, Dept. of Civil and Environmental Engineering, Lehigh Univ., Bethlehem, PA 18015 (corresponding author). E-mail: pakzad@lehigh.edu

[2]Dean, Cockrell School of Engineering, The Univ. of Texas at Austin, Austin, TX 78720.

Note. This manuscript was submitted on February 12, 2008; approved on February 9, 2009; published online on February 25, 2009. Discussion period open until December 1, 2009; separate discussions must be submitted for individual papers. This paper is part of the ***Journal of Structural Engineering***, Vol. 135, No. 7, July 1, 2009. ©ASCE, ISSN 0733-9445/2009/7-863–872/$25.00.

of the ambient vibration data using nonparametric methods. The third section presents the statistical measures used in evaluating the identified vibration modes and a system realization method for optimizing the parameters. The final section presents the statistical properties of the identified vibration modes of the Golden Gate Bridge and compares them with other estimates.

Wireless Sensor Network for Golden Gate Bridge

A wireless sensor network was designed, developed, and deployed to measure and record ambient accelerations of long-span bridges. The network was designed to be scalable in terms of the number of the nodes, complexity of the network topology, data quality, and quantity by addressing integrated hardware and software systems such as sensitivity and range of microelectromechanical-systems (MEMS) sensors, communication bandwidth of the low-power radios, reliability of command dissemination and data transfer, management of large volume of data, and high-frequency sampling (Pakzad et al. 2008). Each node has a sensor board with MEMS accelerometers in two orthogonal directions, a temperature sensor, and a microcontroller and communication mote. The nodes on the main span measure acceleration in vertical and transverse directions. On the tower, the nodes measure acceleration in transverse and longitudinal directions. To study the cost-performance tradeoffs for MEMS accelerometers, each node has two sensors in each direction. The ADXL202 (Analog Devices 1999) accelerometers have a range of ± 2 g. For low-level motion, the Silicon Design 1221 L (Silicon Designs 2007) is used with a range of ± 150 mg. The wireless sensor network is controlled by a high-level program for the TinyOS software platform (Hill et al. 2003). The software architecture and extensions to TinyOS are described in Kim et al. (2007).

Several laboratory and field experiments were performed to determine the robustness, reliability, and performance of the system components. These experiments, described in Pakzad et al. (2005) included static noise characteristic tests to determine the noise floor of the MEMS accelerometers, dynamic range shaking table tests to asses the accuracy of the sensors over a wide frequency range, temperature sensitivity tests, and a variety of field experiments to study the multihop networking and reliable data collection components. Each node was individually calibrated by a rotary tilt table and shift and scale factors for converting the analog to digital converter (ADC) output to acceleration were determined for all accelerometer channels. Fig. 1 shows the results of the static noise tests for one of the prototype nodes. The sensor recorded ambient vibrations at a laboratory environment (McCone Hall) as well as at a vault in Tilden Hill, near University of California Berkeley campus, and the power spectral density for each recording is plotted. The data show that for frequencies above 0.1 Hz, the equivalent root mean square (RMS) acceleration noise is 10 μg. Although the equivalent RMS noise level significantly increases to 80 μg for frequencies lower than 0.1 Hz, the higher noise level is still very low compared with the expected amplitude of the ambient vibrations of a large infrastructure.

For the Golden Gate Bridge, the wireless sensor network consisted of 64 nodes on the main span and the south tower. Fifty six of these nodes were installed on the main span of the bridge, which provide a network that is capable of identifying up to 50 modes in each sensing direction. Considering the low energy of the ambient vibration for higher modes, the density of the network is sufficiently high for an expanded modal analysis of the

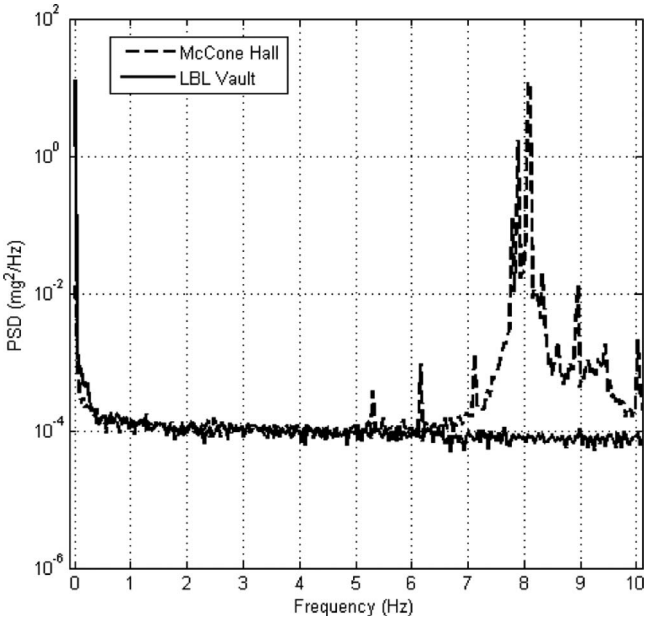

Fig. 1. Zoom plot of noise power spectral density of Silicon Design 1221 sensor at LBL Vault and McCone Lab

bridge. Fig. 2 shows the instrumentation plan for the main span. The nodes on the 1280 m (4,200 ft) main span were located at 30.5 m (100 ft) spacing, but a 15.25 m (50 ft) spacing was used where there was an obstruction hindering radio communication. The eight nodes on the 210 m (745 ft) south tower were placed at the ends of four struts above the roadway. Fifty three nodes were installed beginning on July 10, 2006, on the west side of the main span. On September 15, 2006, the batteries were replaced for the nodes on the main span and three extra nodes were added on the east side. There were a total of 174 data collection runs of the network during the deployment, which lasted until October 14, 2006, including testing and debugging.

The sampling rate for all runs was 1 kHz, but since the significant vibration frequencies of the bridge are much lower, the data were averaged on the node and downsampled to 50 Hz prior to transmission. The averaging is very effective in reducing the noise level and improving the accuracy of the estimated parameters. In some of the runs all five channels on a node (two high-level motion sensors, two low-level motion sensors, and the temperature sensor) were sampled, but in other runs the channels were limited to the low-level accelerometers to reduce the volume of data. Each run generated up to 500 kB data per node, which for the network of 60 nodes produced 30 MB data for 15 million samples. Approximately 1.3 GB data were collected during the deployment of the wireless sensor network on the Golden Gate Bridge.

Power Spectral Analysis of Ambient Vibration Data

Examples of the ambient acceleration records, using the low-level Silicon Design 1221 accelerometers, in the transverse direction of the main span for a typical run are presented in Fig. 3. The amplitude in the transverse direction is generally within 10 mg, with occasional larger peaks caused by moving vehicles. The power spectral densities (PSD) of the acceleration signals using the Welch method (Welch 1967) are shown for frequencies below the

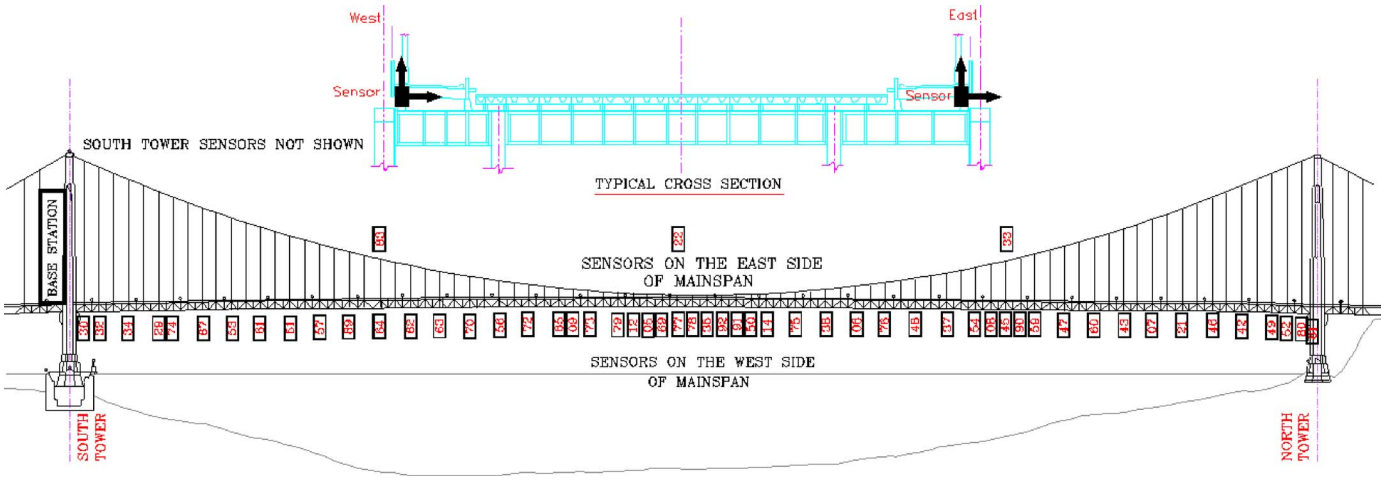

Fig. 2. Instrumentation plan for 56 acceleration sensor nodes on main span of Golden Gate Bridge

25 Hz Nyquist rate. A zoom plot of the lower frequency range has clear peaks at the vibration frequencies of the main span.

The peak picking method is a simple way to estimate modal properties of a system using the PSD of output-only data (Bendat and Piersol 1993). It is based on the property that for a linear system with a white or nearly white noise excitation, the PSD is peaked at the resonant frequencies and the value is proportional to the mode shape, i.e.

$$\phi_{ak} = \alpha S_a(f_k) \tag{1}$$

In Eq. (1), ϕ_{ak} is the ordinate of the k^{th} mode shape Φ_k at location a; and $S_a(f_k)$ is the PSD of the signal at point a evaluated at the k^{th} resonant frequency f_k. When normalized with respect to a reference location, the mode shape is given by the ratio of these PSD values at different locations. Peak picking is not as accurate as methods that consider the cross correlations of the recorded signals, but it can provide a first estimate of vibration properties, and the method is implemented within a sensor network with minimal communication. Fig. 4 shows the lowest identified vertical, transverse, and torsional modes of the main span using peak picking. The lowest vertical mode has a frequency of 0.106 Hz, and the mode shape is antisymmetric, consistent with the expected behavior of a suspension bridge. In the transverse direction the first identified mode is also an antisymmetric mode and the frequency is 0.228 Hz. There is a large low-frequency content in the transverse direction, which is not distinguishable from noise, so the first transverse mode, expected to be symmetric, cannot be identified. Abdel-Ghaffar and Scanlan (1985a) estimated the first symmetric transverse vibration mode with a frequency of 0.055 Hz (18.2 s period). The first identified torsional mode is antisymmetric as expected and it has a frequency of 0.230 Hz. The accuracy of the peak picking method will be assessed using parametric identification methods in a later section of the paper.

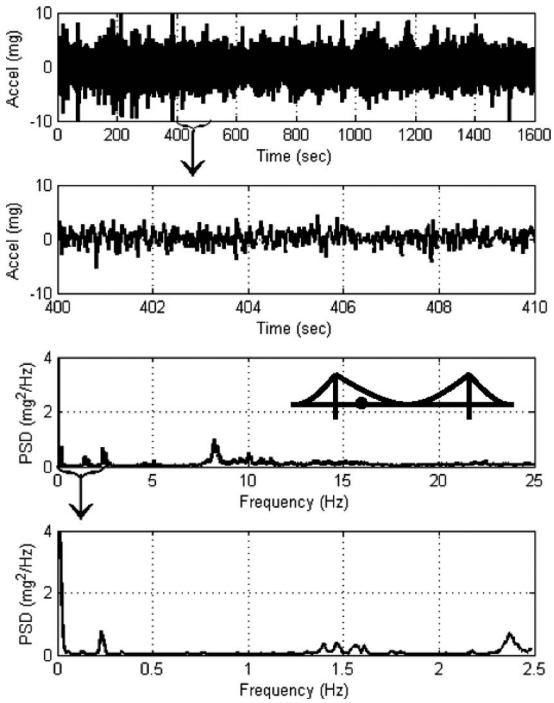

Fig. 3. Time and frequency content of ambient vibration in transverse direction at west side south 1/4 span (Run 174, Node 64)

Modal Identification Method and Statistical Inference

A system identification and statistical analysis of the vibration modes of the bridge is performed using the ambient vibration

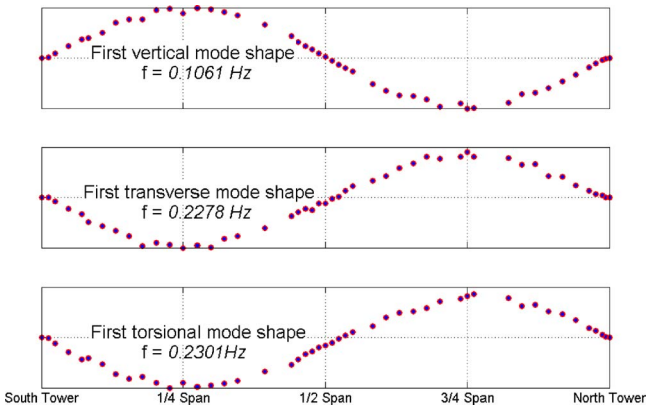

Fig. 4. Nonparametric identification of main span mode shapes using peak picking method (Run 174)

data. In the system identification step the data are used to identify the modal vibration properties. Then this information from multiple runs is used to make statistical inference about the modes and to obtain probabilistic estimates of the modal properties.

System Identification Using Autoregressive with Moving Average Model

An autoregressive with moving average (ARMA) model is used to identify modal properties of the bridge. Pandit (1991) and De Roeck et al. (1995) studied the performance of autoregressive (AR) models for output-only systems and concluded that they give stable, reliable, and accurate results when applied to ambient acceleration measurements. The addition of the moving average noise to the AR model improves the accuracy even further. Andersen (1997) demonstrates the close relation between the ARMA method and subspace identification algorithms and shows that it is a robust and reliable system identification method for linear time-invariant structures subject to unmeasured Gaussian white noise excitation.

With this approach, a dynamic system can be approximated in the discrete time domain by an autoregressive with exogenous term (ARX) model

$$\sum_{i=0}^{M} A_i \bar{y}(n-i) = \sum_{i=1}^{M} B_i \bar{x}(n-i) + \bar{e}(n) \tag{2}$$

In Eq. (2), $\bar{x}(n)=[x_1(n)\ x_2(n)\ \cdots\ x_p(n)]$ and $\bar{y}(n)=[y_1(n)\ y_2(n)\ \cdots\ y_q(n)]$ are p- and q-dimensional input and output vectors and M is the order of the model. For an output-only system, with the assumption of independent and identically distributed (IID) inputs, the unobserved white noise input and measurement error are indistinguishable and thus this system can be approximated by an ARMA model

$$\sum_{i=0}^{M} A_i \bar{y}(n-i) = \sum_{i=1}^{M} \hat{B}_i \bar{e}(n-i) + \bar{e}(n) \tag{3}$$

In Eq. (3), A_i and $\hat{B}_i$ are $q\times q$ and $q\times p$ matrices of autoregressive (AR) and moving-average (MA) coefficients.

The modal parameters of this system can be computed by the eigenvalue decomposition of the corresponding matrix of the AR polynomial

$$S_n = FS_{n-1} + V_n \tag{4}$$

where

$$S_n = \begin{bmatrix} \bar{y}(n) \\ \bar{y}(n-1) \\ \vdots \\ \bar{y}(n-M+1) \end{bmatrix}, \quad V_n = \begin{bmatrix} \sum_{i=1}^{M} \hat{B}_i \bar{e}(n-i) + \bar{e}(n) \\ \bar{0} \\ \vdots \\ \bar{0} \end{bmatrix},$$

$$F = \begin{bmatrix} -A_i & \cdots & -A_{M-1} & -A_M \\ I & \cdots & \bar{0} & \bar{0} \\ \vdots & \ddots & \vdots & \vdots \\ \bar{0} & \cdots & I & \bar{0} \end{bmatrix}$$

The system matrix, F, has eigenvalues Λ and eigenvectors L, and is represented as $F=L\Lambda L^{-1}$, where

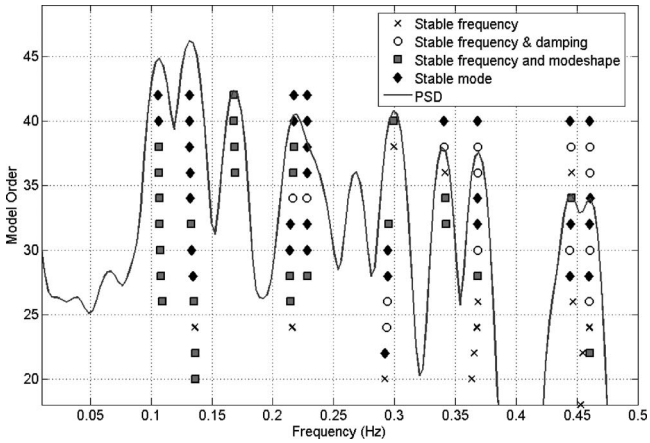

Fig. 5. Stabilization diagram for ARMA model and average PSD as reference (Run 174)

$$L = \begin{bmatrix} \bar{l}_1\lambda_1^{M-1} & \bar{l}_2\lambda_2^{M-1} & \cdots & \bar{l}_{Mq}\lambda_{Mq}^{M-1} \\ \bar{l}_1\lambda_1^{M-2} & \bar{l}_2\lambda_2^{M-2} & \cdots & \bar{l}_{Mq}\lambda_{Mq}^{M-2} \\ \vdots & \vdots & \ddots & \vdots \\ \bar{l}_1 & \bar{l}_2 & \cdots & \bar{l}_{Mq} \end{bmatrix}$$

and $\Lambda=\mathrm{diag}(\lambda_i)$, $i=1,2,\ldots,Mq$.

After the pair $(\lambda_i,\bar{l}_i)$ is estimated, frequency and damping ratios of the continuous-time system are given by

$$\mu_i = \log(\lambda_i), \quad \mu_i,\mu_i^* = -\omega_i\zeta_i \pm j\omega_i\sqrt{1-\zeta_i^2} \Rightarrow \begin{cases} \omega_i = \sqrt{\mu_i\mu_i^*} \\ \zeta_i = \dfrac{\mathrm{Real}(\mu_i)}{\omega_i} \end{cases} \tag{5}$$

The mode shapes are identified from the bottom $q\times Mq$ submatrix of L. The number of identified modes is Mq which is larger than order of a q-degree of freedom (DOF) system. The additional modes are spurious computational modes that result from noise in the signals.

The order of the ARMA model is selected by using stabilization diagrams (Heylen et al. 1995). The stabilization diagram shows the minimum model order that provides enough resolution to identify structural modes but avoids overparameterization of the problem. The computational modes do not repeat consistently, but structural modes stabilize as the order increases. In addition to the stabilization diagrams, two other measures are used to select the structural vibration modes from the ARMA model results. Modal phase collinearity (MPC) (Pappa et al. 1993) is an indicator of monophase behavior of the identified mode shapes. In a noise-free environment, this factor is unity. The presence of noise lowers the MPC, but structural modes still have high values of MPC. In addition, an identified mode should have physically acceptable dynamic properties. A mode with an estimated damping ratio that falls outside an acceptable range cannot be a structural vibration mode.

The three indicators (stabilization diagram, MPC, and damping ratio threshold) are used to identify the vibration frequencies, damping ratios, and mode shapes of the bridge with the ARMA output-only method for each run of the network, and the results are presented in the next section. Modes with a damping ratio greater than 10% or an MPC value less than 0.90 are considered spurious.

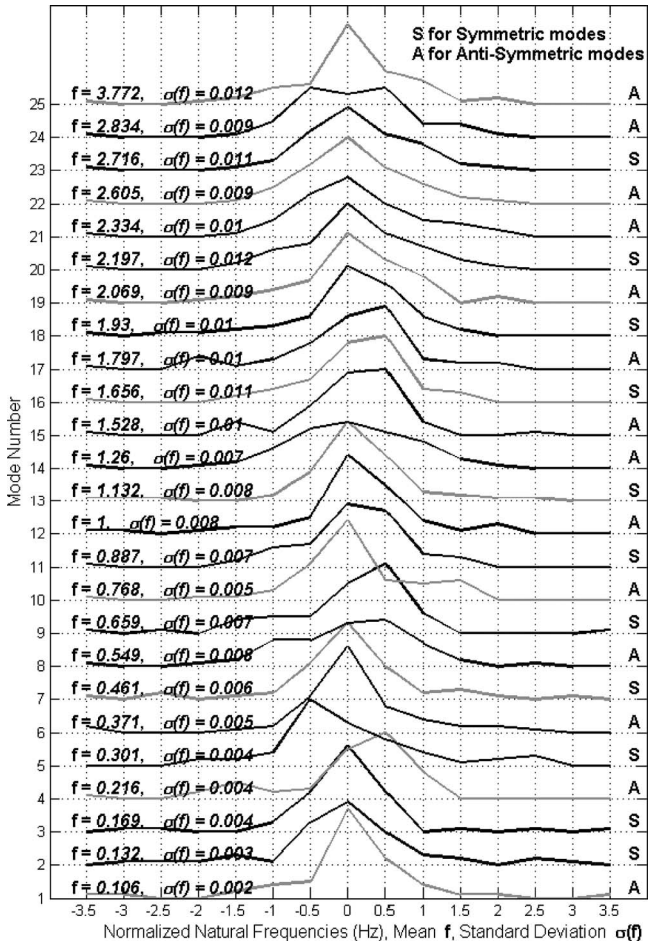

Fig. 6. Histograms of identified vertical vibration frequencies of main span

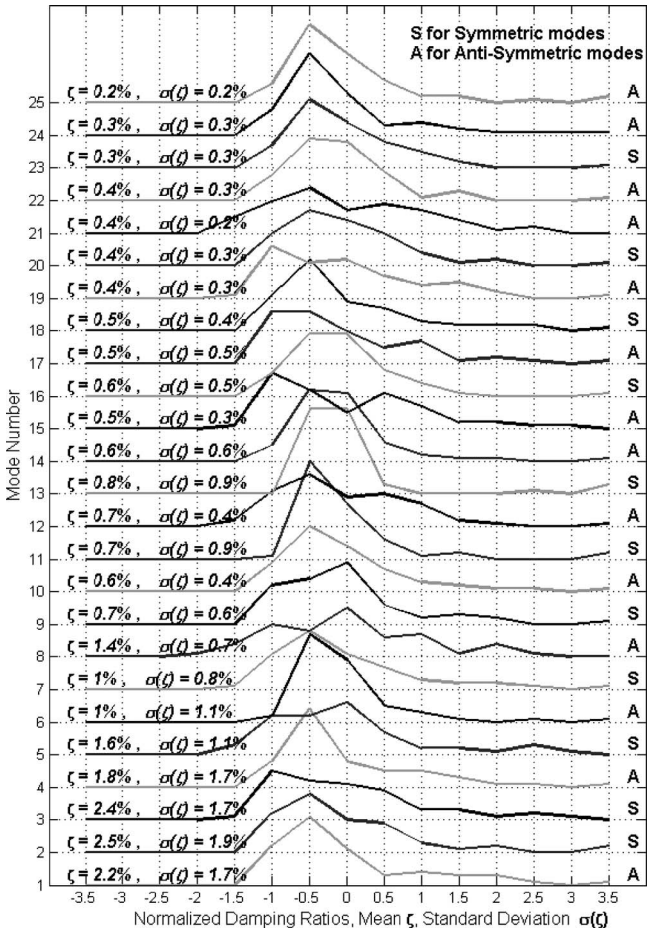

Fig. 7. Histograms of identified vertical damping ratios of main span

Statistical Inference for Identified Vibration Modes

A major advantage of collecting ambient vibration data from many runs is that it is possible to compute statistical measures for the identified vibration modes. The statistical analysis includes histograms and confidence intervals of vibration frequencies, damping ratios, and mode shapes. A histogram is a classical nonparametric estimator of the probability density function (Scott 1979). To examine the distribution of identified parameters, probability plots (Chambers et al. 1983) are used, which are graphical techniques for assessing whether or not a data set is sampled from a particular distribution.

For the mode shapes, as well as the frequencies and damping ratios, the statistics are also presented by the mean value of the parameters and their confidence intervals (CIs). A 95% CI for a point-estimated parameter can be interpreted as an interval that is believed, with 95% confidence, to include the true value of the parameter. In other words, if the same procedures are repeated (sampling from the population, estimating the parameter, and finding CIs), 95% of the times the estimated CIs are expected to include the true value of the parameter.

This statistical analysis allows inference about the certainty of the estimation of modal vibration properties. The narrower the histograms or confidence intervals are, the less uncertainty the estimated values have. The approach can also be used as a comparison basis for other estimations of the same modal parameters. A new estimate that lies inside the CI is consistent with the hypothesis that no change has occurred. If it falls outside the interval, the inconsistency can be explained by either the fact that the underlying parameter has changed, or that the new estimate is not an accurate estimate of the underlying parameter, or that the CI is not an accurate CI and does not include the true value of the parameter. Each of these could be a valid explanation and should be explored, considering other information about the estimation process and physical model.

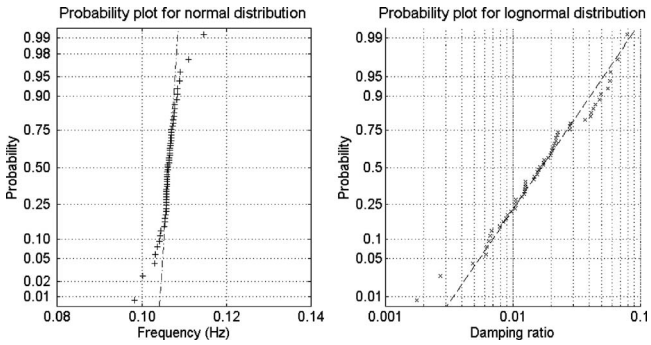

Fig. 8. Normal probability plots for frequencies and damping ratios of first identified vertical mode

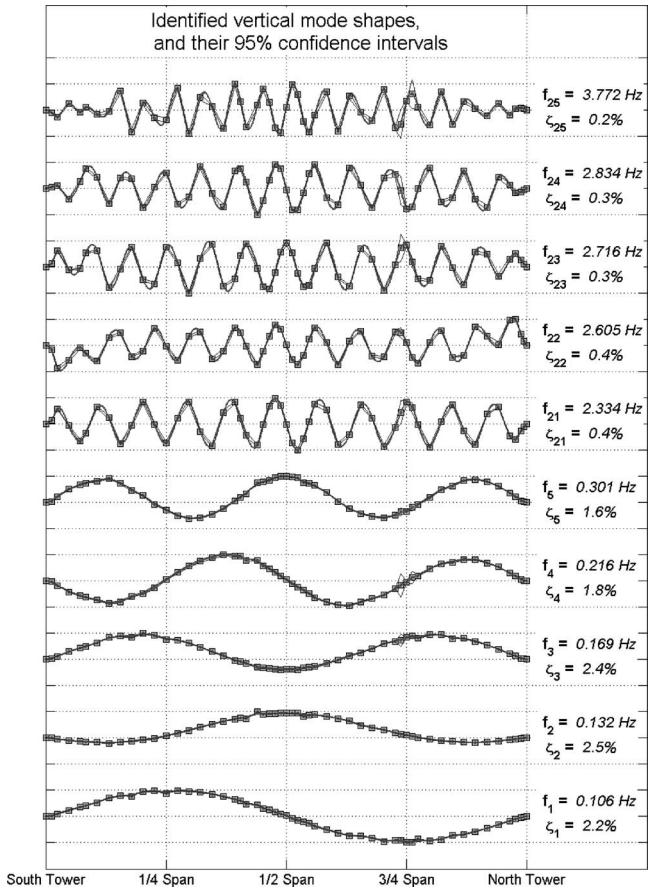

Fig. 9. Identified five lowest and highest frequency vertical mode shapes of main span and their 95% confidence intervals

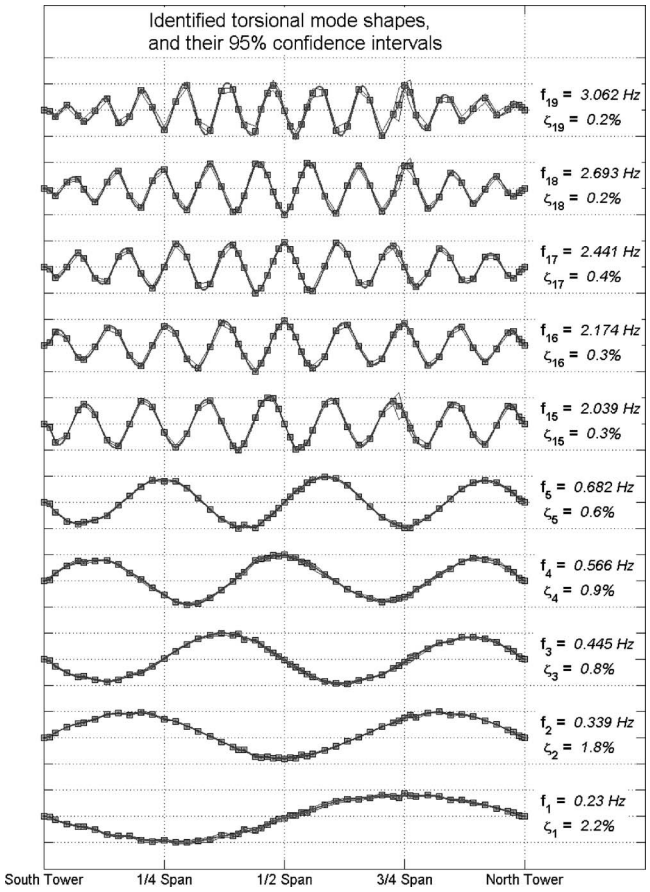

Fig. 10. Identified five lowest and highest frequency torsional mode shapes of main span and their 95% confidence intervals

Statistical Analysis of Vibration Modes

The application of the statistical approach for the vibration modes of the Golden Gate Bridge is presented in this section. The vibration frequencies, damping ratios, and mode shapes for the main span are identified using the methodology presented in the previous section for data from all 174 runs of the network. The confidence intervals are then compared with the results from other methods to make statistical inference about the accuracy of the identified vibration modes.

System Identification

The ambient acceleration signals are low-pass filtered with a Chebychev Type-II filter with 5 Hz cutoff. The ARMA method and stabilization graphs are used to determine the order of the model and select the structural vibration modes. A typical stabilization diagram for determining the model order and selecting the vertical modes using the data from one run (174) is shown in Fig. 5. Each point on the diagram represents an identified mode. A horizontal row of the diagram gives the identified modes using a particular model order, and the vertical columns show the evolution of an identified mode as the model order increases. An "*x*" in the plot represents a mode that has stable frequency, i.e., the relative difference of the identified frequency compared with that of the same mode using a lower model order is within 1%. If both identified frequency and damping ratio are stable, the mode is represented by an "*o*." The average PSD of the signals for all nodes is also plotted on the same figure as the reference, and is used to confirm that the identified vibration frequencies correspond to the peaks of PSD. Based on this typical diagram, for example, a model order of 40 is necessary to achieve stable modes up to 0.50 Hz.

Statistical Analysis

The results of system identification are used to estimate statistical properties of vibration frequencies, damping ratios, and mode shapes for the vertical, torsional, and transverse modes of the main span. The histograms for vibration frequencies and damping ratios are plotted with the mean value centered at the origin over a range of ± 3.5 times the standard deviation. Figs. 6 and 7 show the histograms of the vibration frequencies and damping ratios for the modes in vertical direction (the histograms of the frequencies and damping ratios for transverse and torsional modes are omitted due to space limitation). Twenty five vertical, 19 torsional, and 23 transverse modes with frequencies less than 5 Hz are identified. The vertical axes of the graphs are the identified mode numbers. The mean and standard deviation of the estimated parameters are listed for each mode. Each histogram is marked with an "A" for the antisymmetric modes or an "S" for the symmetric ones.

Fig. 8 shows typical normal and lognormal probability plots for the frequencies and damping ratios. The horizontal axis is the data values and the vertical axis is the probability values scaled to normal or lognormal distribution. Each sample is represented by a plus sign that shows the empirical probability versus the data value for that data point. A data set sampled from a normal (or lognormal) distribution produces points that follow a straight line

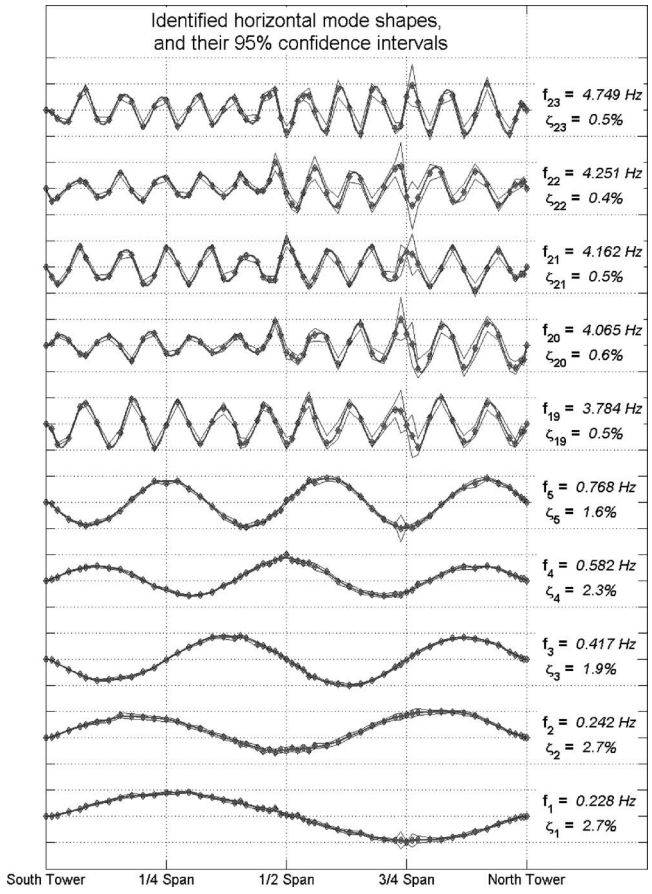

Fig. 11. Identified five lowest and highest frequency transverse mode shapes of main span and their 95% confidence intervals

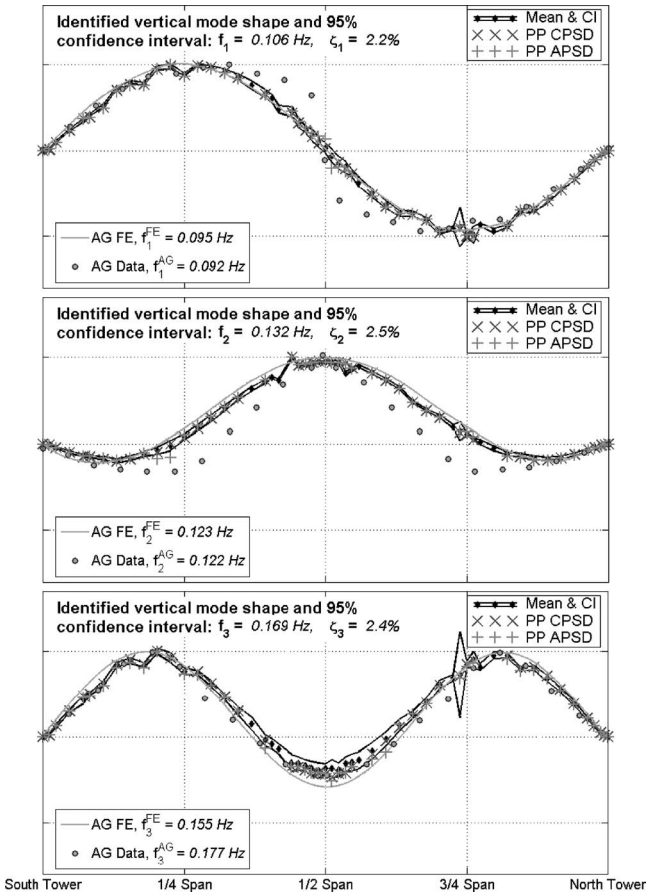

Fig. 12. Comparison between lowest three identified vertical mode shape using ARMA method, peak picking method, 1982 data from Abdel-Ghaffar test, and 1982 finite-elements model by Abdel-Ghaffar

in the normal (or lognormal) probability graph. The left-hand side normal probability graph for the first vertical frequency shows a linear behavior in the middle part, but an s-shape deviation on the tails, indicating shorter than normal tails. This means that the variance of the data is less than expected for a normal distribution. The right-hand side lognormal probability graph is for the damping ratio of the first vertical mode, and again, the middle part of the plot is close to linear. The tails behavior is also consistent with the straight line, confirming that the distribution is close to lognormal as expected. The probability plots are used to evaluate the assumption of normality for the measurement noise and modeling error. In this case, the distributions of identified parameters are close to normal for frequencies and lognormal for the damping ratios, which validate the model assumptions. They also serve to validate distribution assumptions for hypothesis testing using estimated parameters, i.e., confidence intervals for the modal parameters can be constructed assuming that the parameters have normal or lognormal distributions.

The mean value and 95% confidence intervals for vibration frequencies and damping ratios for the vertical modes are presented in Table 1 (the presented results are limited to the vertical modes due to space limitation; in addition, statistical properties of the transverse and torsional modes were obtained). For mode shapes, the mean value and 95% confidence intervals of each node for the lowest and highest five identified modes in each direction are plotted in Figs. 9–11. The confidence intervals are small for both lower and higher mode shapes, which is an indication of the high quality of data within the frequency range up to 5 Hz.

The identified mode shapes are generally consistent with the dynamic properties of a long-span suspension bridge. In the vertical direction the first symmetric mode is at a frequency higher than the first antisymmetric mode due to the arch effect of the cables (Henrych 1981). In the transverse direction however, the first symmetric mode, which is expected to have a lower frequency than the first antisymmetric mode, is not identified with the sensor network. As mentioned earlier, the power spectral densities of the transverse signals in Fig. 3 indicate that the frequency content of the signals at very low frequencies are indistinguishable from the accelerometer noise floor. As a result, the signal to noise ratio is low in the very low frequency range, so it is not possible to identify this mode from ambient vibration with the inexpensive sensors.

The confidence intervals of several mode shapes at the two locations near the 3/4-span are wider than usual. The nodes at these locations were added in the second phase of deployment and those nodes collected a limited number of data. When the noise level at a frequency is high, the identified mode shapes have a higher variance at these locations, which results in wide confidence intervals.

Comparison of Vibration Modes

The statistical results for the vibration modes of the Golden Gate Bridge, along with the confidence intervals in the current study, can be used to assess the three sets of identified vibration modes

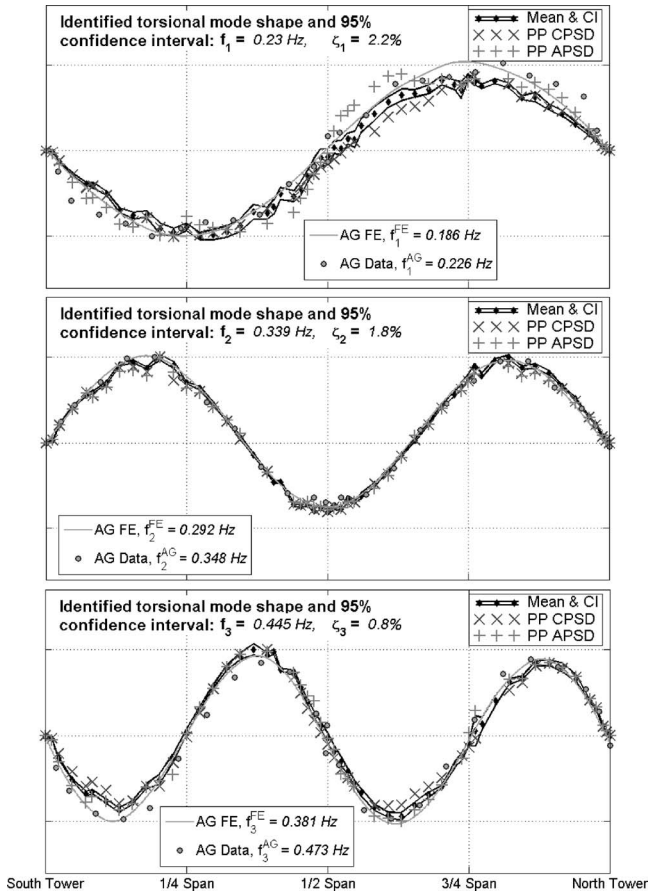

Fig. 13. Comparison between lowest three identified torsional mode shape using ARMA method, peak picking method, 1982 data from Abdel-Ghaffar test, and 1982 finite-elements model by Abdel-Ghaffar

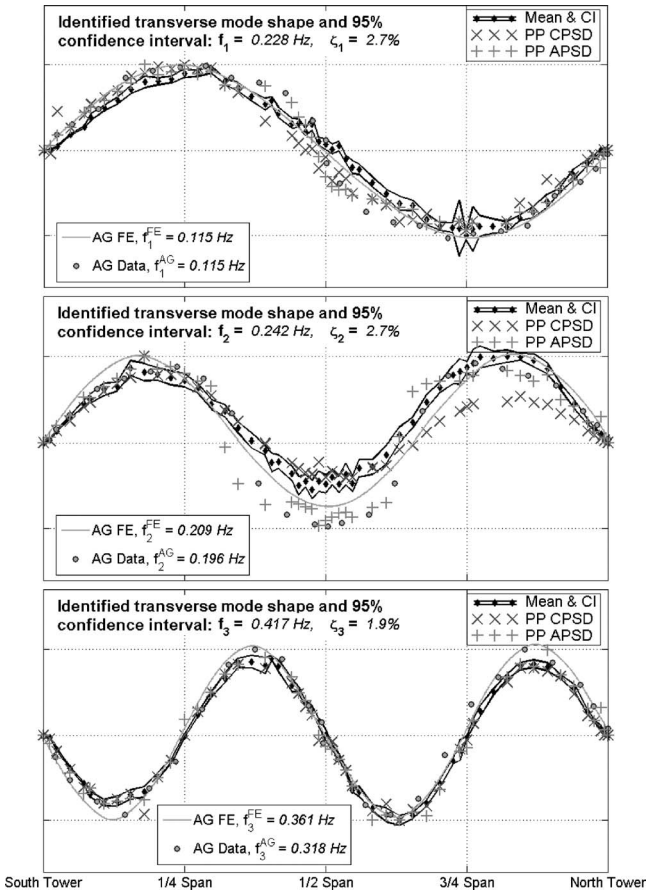

Fig. 14. Comparison between lowest three identified transverse mode shape using ARMA method, peak picking method, 1982 data from Abdel-Ghaffar test, and 1982 finite-elements model by Abdel-Ghaffar

from previous studies. Abdel-Ghaffar and Scanlan (1985a) used sensors on the south side of the main span and the south tower of the Golden Gate Bridge. On the main span, six accelerometers, two in each direction, were installed at a location near the south 1/4-span as the reference station. Another group of six accelerometers were moved from station to station at 18 locations and the spectral amplitude of each was compared with that of the reference station to identify the vibration modes of the bridge. This is a peak picking method, in that the relative spectral amplitudes at peak frequencies are used to estimate the mode shapes, but since the data were not collected simultaneously it can produce large errors. Two-dimensional finite-element models of the bridge were also used to compute vibration modes (Abdel-Ghaffar and Rubin 1983a,b,c and Abdel-Ghaffar et al. 1985).

To evaluate the peak picking method, the power spectral densities at peak frequencies are used to estimate the mode shapes using the data from 54 nodes in the wireless sensor network for one run (#174). Figs. 12–14 show the lowest three identified vertical, transverse, and torsional modes. The first three vertical mode shapes from peak picking lie within the confidence intervals, which confirms the accuracy of the simplified method. For the second and third torsional modes [Figs. 13(b and c)] and the third transverse mode [Fig. 14(c)], the peak picking results are also within the confidence intervals. In three cases, however, the peak picking results are outside the confidence intervals [first torsional in Fig. 13(a), and first and second transverse in Figs. 14(a and b)]. This is because the three modes have relatively close frequencies (0.228, 0.230, and 0.242 Hz), and the peak picking method is most accurate when the peak frequencies are well separated. The identified vibration modes by Abdel-Ghaffar and Scanlan (1985a) are generally similar to the statistical analysis of the data from the wireless sensor network. Several of the mode shape ordinates, however, are outside the confidence intervals. In this comparison, it must be recognized that the bridge has been retrofitted since the earlier data were collected including a complete replacement of the roadway deck. This comparison indicates that the earlier estimates of mode shapes are not very accurate because of the change in the main span, but also because of the quality of the data and the error in the system identification method for the earlier estimates. The 1985 data best match the confidence intervals for vertical Mode 3 [Fig. 12(c)], torsional Modes 2 and 3 [Figs. 13(b and c)], and transverse Mode 3 [Fig. 14(c)], indicating that the change in dynamic properties of the bridge most effected the low-frequency modes.

In the case of the finite-element model developed by Abdel-Ghaffar et al. (1985), all the modes except for the second transverse mode fall within the confidence intervals. The confidence intervals for second transverse mode are wider than the other modes, and have a larger spatial variation, suggesting that the collected data are noisier at this frequency, which has resulted in confidence intervals that are less accurate.

Table 1. Mean Values and 95% Confidence Bounds (CB) for Frequencies and Damping Ratios of Golden Gate Bridge Vertical Modes

	Frequency (Hz)			Damping ratio (%)		
Mode	Mean	Lower CB	Upper CB	Mean	Lower CB	Upper CB
1 A	**0.1065**	*0.1060*	*0.1070*	**2.1**	*1.7*	*2.6*
2 S	**0.1322**	*0.1315*	*0.1330*	**2.4**	*2.0*	*2.9*
3 S	**0.1696**	*0.1686*	*0.1706*	**2.3**	*1.9*	*2.7*
4 A	**0.2165**	*0.2156*	*0.2174*	**1.6**	*1.3*	*2.0*
5 S	**0.3010**	*0.2999*	*0.3021*	**1.6**	*1.3*	*1.9*
6 A	**0.3709**	*0.3697*	*0.3721*	**0.8**	*0.7*	*1.0*
7 S	**0.4609**	*0.4595*	*0.4624*	**1.0**	*0.8*	*1.2*
8 A	**0.5498**	*0.5480*	*0.5517*	**1.4**	*1.2*	*1.6*
9 S	**0.6592**	*0.6577*	*0.6608*	**0.7**	*0.6*	*0.8*
10 A	**0.7686**	*0.7676*	*0.7696*	**0.6**	*0.5*	*0.7*
11 S	**0.8874**	*0.8862*	*0.8885*	**0.7**	*0.5*	*1.0*
12 A	**1.0002**	*0.9984*	*1.0020*	**0.7**	*0.6*	*0.9*
13 S	**1.1321**	*1.1303*	*1.1339*	**0.8**	*0.5*	*1.0*
14 A	**1.2608**	*1.2594*	*1.2623*	**0.6**	*0.4*	*0.7*
15 A	**1.5289**	*1.5272*	*1.5306*	**0.5**	*0.4*	*0.6*
16 S	**1.6571**	*1.6552*	*1.6590*	**0.6**	*0.4*	*0.7*
17 A	**1.7974**	*1.7951*	*1.7996*	**0.5**	*0.4*	*0.7*
18 S	**1.9308**	*1.9289*	*1.9327*	**0.5**	*0.4*	*0.6*
19 A	**2.0702**	*2.0685*	*2.0719*	**0.4**	*0.3*	*0.4*
20 S	**2.1980**	*2.1956*	*2.2003*	**0.4**	*0.3*	*0.5*
21 A	**2.3352**	*2.3333*	*2.3372*	**0.4**	*0.3*	*0.4*
22 A	**2.6060**	*2.6043*	*2.6076*	**0.4**	*0.3*	*0.4*
23 S	**2.7172**	*2.7152*	*2.7192*	**0.3**	*0.2*	*0.4*
24 A	**2.8353**	*2.8337*	*2.8370*	**0.3**	*0.2*	*0.4*
25 A	**3.7727**	*3.7705*	*3.7749*	**0.3**	*0.2*	*0.3*

Note: Lower CB = lower confidence bound; A = antisymmetric mode; Upper CB = upper confidence bound; and S = symmetric mode.

Conclusions

The 3-month deployment of a spatially dense wireless accelerometer sensor network on the main span of the Golden Gate Bridge provided valuable vibration data in vertical and transverse directions. The data were analyzed using the peak picking method, and then using an ARMA model. The vibration modes of the main span were identified, and statistical properties of the modes were determined from a series of data runs. For vibration frequencies and damping ratios, histograms and confidence intervals of the identified parameters were presented, which show an estimate of the distribution and provide a measure of variability in identification process.

For the mode shapes, the 95% confidence intervals are determined to provide a high level of certainty in the identified vibration modes. The standard deviations of the frequencies range from about 2% of the mean for the lower modes to 0.2% for higher modes. The damping ratios have more variability, as the standard deviations are sometimes as high as the mean of the identified parameters. The confidence intervals for the mode shapes also show a high level of certainty in identified shapes. These tight confidence intervals are repeated throughout the spectrum, and the higher vibration mode shapes are also identified with high confidence level. Overall 25 modes in vertical direction, 23 in transverse direction, and 19 torsional modes were identified in the 0–5 Hz frequency range.

The identified modes were compared with the peak picking results and the findings of a previous study on the bridge, where both acceleration data and finite-element models were used in estimating the modal properties of the bridge. A comparison of the first three modes in each direction shows that the mode shapes from spectral method (peak picking) and finite-element models generally agree with the findings of this paper. The observation that peak picking results match the statistical analysis suggests that for the long-span bridges, when the goal of the analysis is estimation of the modal properties, the simpler and faster system identification method of peak picking is sufficient. The peak picking algorithm could be implemented in a wireless network to distribute the system identification analysis, which in turn could reduce the communication load of the a n-node linear network by a factor of up to $(n+1)/2$. The identified mode shapes resulting from the earlier data collection fall outside the 95% confidence intervals in the lower modes, which can be explained by changes in dynamic properties of the bridge after redecking and retrofitting, and the identification method used to estimate the mode shapes.

High spatial density of the scalable wireless sensor network provided a high resolution for the spatial aspects of dynamic behavior of the bridge. The robustness of the system made it easy to collect multiple realizations of data sets, which were used for assessing the integrity and accuracy of identified parameters, and gave a statistical platform for evaluating other estimates of the same parameters.

Acknowledgments

This work reflects the advice and guidance of Professor James Demmel, Professor Steven Glaser, and Professor David Culler

who participated and supported the research. Dr. Sukun Kim developed the software and closely collaborated in design of hardware and deployment of the network on the Golden Gate Bridge. The writers give special thanks to the staff and management of the Golden Gate Bridge, Highway and Transportation District, in particular, Dennis Mulligan and Jerry Kao, for their close cooperation in every step of the project. Jorge Lee provided extraordinary help in the deployment, which made this project possible. Tom Oberheim helped design and develop the sensor board. This research was supported by the National Science Foundation under Grant No. EIA-0122599 and by the Center for Information Technology Research in the Interest of Society (CITRIS) at the University of California, Berkeley.

References

Abdel-Ghaffar, A. M., Masri, S. F., and Nigbor, R. N. (1995). "Preliminary report on the Vincent Thomas Bridge monitoring test." *Center for Research in Earthquake and Construction Engineering, Rep. No. M9510*, Univ. of Southern California, Los Angeles.

Abdel-Ghaffar, A. M., and Rubin, L. I. (1983a). "Lateral earthquake response of suspension bridges." *J. Struct. Eng.*, 109(3), 664–675.

Abdel-Ghaffar, A. M., and Rubin, L. I. (1983b). "Nonlinear free coupled vertical-torsional vibrations of suspension bridges. Part II: Application." *J. Eng. Mech.*, 109(1), 330–345.

Abdel-Ghaffar, A. M. and Rubin, L. I. (1983c). "Vertical seismic behavior of suspension bridges." *Earthquake Eng. Struct. Dyn.*, 11 (Jan.–Feb.), 1–19.

Abdel-Ghaffar, A. M., and Scanlan, R. H. (1985a). "Ambient vibration studies of Golden Gate Bridge. I: Suspended structure." *J. Eng. Mech.*, 111(4), 463–482.

Abdel-Ghaffar, A. M., and Scanlan, R. H. (1985b). "Ambient vibration studies of Golden Gate Bridge. II: Pier-tower structure." *J. Eng. Mech.*, 111(4), 483–499.

Abdel-Ghaffar, A. M., Scanlan, R. H., and Diehl, J. (1985). "Analysis of the dynamic characteristics of the Golden Gate Bridge by ambient vibration measurements." *Rep No. 85-SM-1*, Dept. of Civil Engineering, Princeton Univ. Princeton, N.Y.

Analog Devices. (1999). "ADXL202/ADXL210: Low cost ±2 g/ ±10 g dual axis iMEMS→ Accelerometers with digital output data sheet." ⟨http://www.analog.com/en/prod/0,2877,ADXL202,00.html⟩.

Andersen, P. (1997). "Identification of civil engineering structures using vector ARMA models." Ph.D., Dept. of Building Technology and Structural Engineering, Aalborg Univ., Aalborg, Denmark.

Bendat, J. S., and Piersol, A. G. (1993). *Engineering applications of correlation and spectral analysis*, 2nd Ed., Wiley, New York.

Brownjohn, J. M. W., Dumanoglu, A. A., and Severn, R. T. (1992). "Ambient vibration survey of the Fatih Sultan Mehmet (Second Bosporus) Suspension Bridge." *Earthquake Eng. Struct. Dyn.*, 21, 907–924.

Brownjohn, J. M. W., Dumanoglu, A. A., Severn, R. T., and Blakeborough, A. (1989). "Ambient vibration survey of the Bosporus Suspension Bridge." *Earthquake Eng. Struct. Dyn.*, 18, 263–283.

Chambers, J., Cleveland, W., Kleiner, B., and Tukey, P. (1983). "Graphical methods for data analysis." Wodsworth Int. Group, Belmont, Calif., and Duxbury Press, Boston.

Chang, C. C., Chang, T. Y. P., and Zhang, Q. W. (2001). "Ambient vibration of long-span cable-stayed bridge." *J. Bridge Eng.*, 6(1), 46–53.

Cunha, A., Caetano, E., and Delgado, R. (2001). "Dynamic tests on large cable-stayed bridge." *J. Bridge Eng.*, 6(1), 54–62.

De Roeck, G., Claesen, W., and Van Den Broeck, P. (1995). "DDS-methodology applied to parameter identification of civil engineering structures." *Proc., Vibration and Noise '95*, Venice, Italy, 341–353.

Fujino, Y., et al. (2000). "Forced and ambient vibration tests and vibration monitoring of Hakucho Suspension Bridge." *Transportation Research Record. 1696*, Transportation Research Record, Washington, D.C., A57-A63.

Grimmelsman, K. A., Pan, Q., and Aktan, A. E. (2007). "Analysis of data quality for ambient vibration testing of the Henry Hudson Bridge." *J. Intell. Mater. Syst. Struct.*, 18, 765–775.

He, X., et al. (2005). "System identification of New Carquinez bridge using ambient vibration data." *Proc., Int. Conf. on Experimental Vibration analysis of Civil Engineering Structures*, France, 26–28.

Henrych, J. (1981). *The dynamics of arches and frames*, Elsevier, Amsterdam, The Netherlands.

Heylen, W., Lammens, S., and Sas, P. (1995). "Modal analysis theory and testing." Dept. of Mechanical Engineering, Katholieke Univ. Leuven, Leuven, Belgium.

Hill, J., Gay, D., and Levis, P. (2003). ⟨http://www.tinyos.net/tinyos-1.x/tos/system⟩.

Jones, N. P., and Spartz, C. A. (1990). "Structural damping estimation for long-span bridges." *J. Eng. Mech.*, 116(11), 2414–2433.

Kim, S., et al. (2007). "Health monitoring of civil infrastructures using wireless sensor networks." *Proc., 6th Int. Conf. on Information Processing in Sensor Networks (IPSN)*, Cambridge, Mass.

Lu, K. C., et al. (2006). "Ambient vibration study of Gi-Lu cable-stay bridge: application of wireless sensing units." *Proc. SPIE*, 6174, 419–429.

Niazy, A. M. (1991). "Seismic performance evaluation of suspension bridges." Ph. D., Univ. of Southern California, Los Angeles.

Pakzad, S. N., Fenves, G. L., Kim, S., and Culler, D. E. (2008). "Design and implementation of scalable wireless sensor network for structural monitoring." *J. Infrastruct. Syst.*, 14(1), 89–101.

Pakzad, S. N., Kim, S., Fenves, G. L., Glaser, S. D., Culler, D. E., and Demmel, J. W. (2005). "Multi-purpose wireless accelerometers for civil infrastructure monitoring." *Proc., 5th Int. Workshop on Structural Health Monitoring (IWSHM 2005)*, Stanford, Calif.

Pandit, S. M. (1991). *Modal and spectrum analysis: Data dependent systems in state space*, Wiley, New York.

Pappa, R. S., Elliott, K. B., and Schenck, A. (1993). "Consistent mode indicator for eigen system realization algorithm." *J. Guid. Control Dyn.*, 16(5), 852–858.

Scott, D. W. (1979). "On optimal and data-based histograms." *Biometrika*, 66(3), 605–610.

Silicon Designs (2007). "Low noise analog accelerometer." ⟨http://www.silicondesigns.com/Pdf/1221.pdf⟩.

Smyth, A. W., Pei, J. S., and Masri, S. F. (2003). "System identification of the Vincent Thomas Suspension Bridge using earthquake records." *Earthquake Eng. Struct. Dyn.*, 32, 339–367.

Stahl, F. L., Mohn, D. E., and Currie, M. C. (2007). "The Golden Gate Bridge." *Rep. of the Chief Engineer*, Vol. II, Golden Gate Bridge and Transportation District, San Francisco.

Strauss, J. B. (1937). "The Golden Gate Bridge." *Rep. to the Board of Directors of the Golden Gate Bridge and Highway District*, Calif.

Vincent, G. S. (1958). "Golden Gate Bridge vibration studies." *Trans. Am. Soc. Civ. Eng.*, 127(11), 667–707.

Vincent, G. S. (1962). "Correlation of predicted and observed suspension bridge behavior." *Trans. Am. Soc. Civ. Eng.*, 127(PII), 646–666.

Welch, P. D. (1967). "The use of fast Fourier transform for the estimation of power spectra: A method based on time averaging over short, modified periodograms." *IEEE Trans. Audio Electroacoust.*, 15(2), 70–73.